Oceanic biological productivity

CHARLES R. McCLAIN, GENE FELDMAN AND WAYNE ESAIAS

Introduction

Microscopic green plants, called phytoplankton, form the lowest trophic level of the marine food web and play important roles in many geochemical processes. Through photosynthesis, they convert dissolved CO_2 and other dissolved nutrients into organic and other metabolic compounds which initiate additional pathways in the biogeochemical cycles of elements such as carbon, nitrogen, phosphorus, oxygen and sulfur. Each cycle consists of processes that couple the terrestrial, atmospheric and oceanic domains and includes feedback mechanisms which modulate the interactions between the various cycle components. Furthermore, cycles are intimately linked, in ways not well understood, so that perturbations in one cycle propagate into the others. A more fundamental understanding of biogeochemical cycles is essential in quantifying man's impact on the global biosphere and poses a fascinating challenge to the earth science community.

With respect to 'global change', the carbon cycle is of particular interest (Sundquist & Broecker, 1985). Fig. 1 is a simplified flow diagram of the global carbon cycle with current estimates of reservoir sizes and flux rates (Moore & Bolin, 1986). The flux pathways (arrows) represent various processes such as photosynthesis and respiration. The figure indicates that 'ocean biota' (primarily phytoplankton and zooplankton) represent a small fraction of the total carbon in the system, but that the associated fluxes are similar in magnitude to those linked with other much larger reservoirs. Thus, the relative turnover rate (flux/reservoir size) of the ocean biota component is very large compared to the others, implying that phytoplankton are a very 'active' component of the system. Indeed, phytoplankton doubling rates are on the order of once/day. Therefore, phytoplankton should respond rapidly to changes in the equilibrium of biogeochemical systems and may play an important role in the readjustment process. The recent rapid increase in atmospheric CO_2 is one case where an observable response might be expected. However, because phytoplankton concentrations and the rates of photosynthesis are controlled by environmental and physiological conditions which are, in turn, coupled to a variety of physical, chemical and other biological variables, the unambiguous identification of a response may not be straightforward.

The fixation of carbon by plants or primary productivity (Falkowski, 1980), Π, is commonly quantified in units of mg $C/m^2/day$. It is the total mass of carbon transformed from dissolved CO_2 to organic carbon integrated throughout the water column per unit area per unit time. Estimates of global primary productivity have been compiled by a number of authors based on historical data (see Berger, 1989). These composites are climatologies derived from available shipboard observations and, therefore, do not resolve seasonal and inter-annual variability or long-term trends on basin and global scales. Also, the estimates were obtained using a number of different techniques of varying accuracy (Eppley, 1989), and the data density in areas such as the Southern Hemisphere is very sparse. Much of the productivity is sustained through the recycling of nutrients within the euphotic zone and is called 'regenerated production'. Any additional production resulting from nutrient fluxes, primarily nitrate, into the euphotic zone is called 'new production' and the proportion of new production to the primary production is the '*f*-ratio'. One equation for the non-dimensional *f*-ratio is

$$f = \Pi/1096 - \Pi^2/2.55*10^6, \quad (1)$$

where Π is the primary productivity given in mg $C/m^2/day$ (Berger, Smetacek & Wefer, 1989). This relation is valid for values less than 1400 mg $C/m^2/day$. Assuming that the partial pressure of CO_2, pCO_2, is approximately in equilibrium with the atmosphere, any increase in phytoplankton uptake will result in a CO_2 flux into the ocean. Associated with primary production is 'export production', primarily in the form of particulate organic carbon (POC; fecal pellets and shells), which is the loss due to sinking. Export production decreases with depth as a result of: 1) oxidation of POC into dissolved organic carbon (DOC) by bacteria and 2) the increase in $CaCO_3$ solubility with depth. Sediment traps are commonly used to measure export production and have demonstrated the link between surface productivity and particle fluxes at

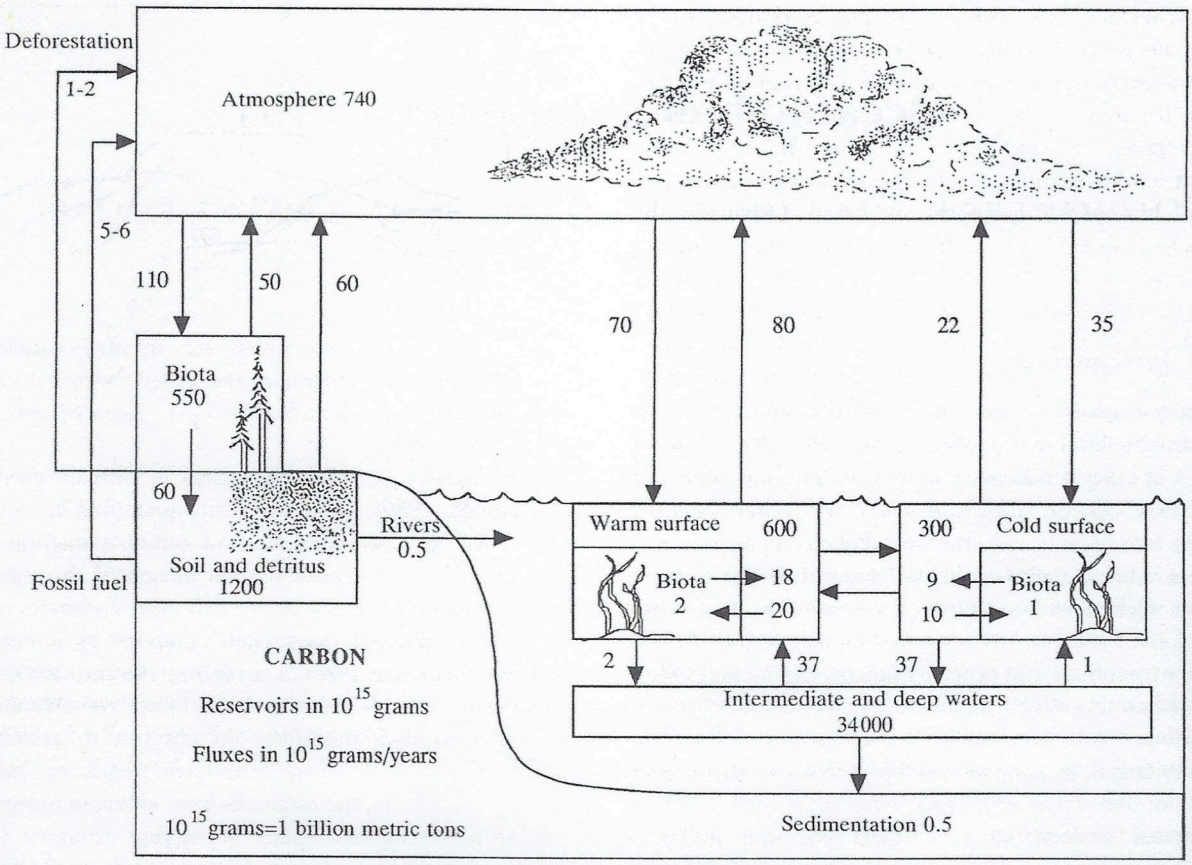

Fig. 1. Schematic of the global carbon cycle with current estimates of reservoir sizes and fluxes (redrawn from Moore & Bolin, 1986).

depth (Deuser, Muller-Karger & Hemleben, 1988). The process of CO_2 uptake in the euphotic zone and its removal to the deep ocean is referred to as the 'biological pump'. In regions where vertical processes dominate nutrient transport, new production and export production are balanced under steady-state conditions.

It has been estimated that only half of the CO_2 released into the atmosphere from the combustion of fossil fuels has remained in the atmosphere. Much of the remainder is thought by many to have been absorbed by the ocean, presumably through the actions of deep water formation and the biological pump. However, neither process is well understood and the role of the ocean in sequestering excess CO_2 is being questioned (Tans, Fung & Takahashi, 1990). An early review of the ocean's role in the fossil fuel CO_2 issue is provided in Anderson and Malahoff (1977). In order to clarify better the production and fate of biogenic materials in the ocean, the Joint Global Ocean Flux Study (JGOFS; Global Ocean Flux Committee, 1984) has been initiated. This experiment requires global long-term observations of phytoplankton biomass and other geophysical quantities, some of which can be estimated from space-borne instrumentation. The first JGOFS field experiment was conducted in the spring of 1989 and was designed to document the onset and development of the North Atlantic spring bloom. The second field experiment will be conducted in the tropical Pacific Ocean in 1992 and a third is being planned for the Indian Ocean.

Methodology

The Coastal Zone Color Scanner mission, algorithms and processing

Because of the great variability of phytoplankton, it is not feasible to collect sufficient amounts of *in situ* data to quantify phytoplankton biomass over large time- and space scales. The Nimbus-7/Coastal Zone Color Scanner (CZCS) was designed as a one-year proof-of-concept experiment to determine if space-borne sensors could provide reasonable estimates of surface pigment concentration (chlorophyll-a

plus phaeophytin) and diffuse attenuation (Hovis, 1981). Because the atmosphere produces roughly 90% of the radiation (molecular plus aerosol scattering) received by a spaceborne instrument viewing the open ocean, it was unclear if these components could be removed with sufficient accuracy to extract reliable estimates of the water-leaving radiances on which all bio-optical algorithms are based. Originally, the plan was to process 1% of the data to level-2 products (water-leaving radiances at 443 nm, 520 nm and 550 nm, aerosol radiance at 670 nm, pigment concentration and diffuse attenuation at 490 nm). However, because of the subsequent success in the development of atmospheric correction (Gordon *et al.*, 1983*a*; Gordon, Brown & Evans, 1988) and bio-optical algorithms (Clark, 1981) and the sensor's extended operation (October 1978 through June 1986), a global processing effort was initiated in 1985 (Esaias *et al.*, 1986; Feldman *et al.*, 1989) and completed in early 1990. This data set has provided the first glimpse of global scale variability on monthly, seasonal and inter-annual time scales and the CZCS has been very useful in a number of specific process-oriented studies (McClain, Pietrafesa & Yoder, 1984; Feldman, Clark & Halpen, 1984; Abbott & Zion, 1985; Barale, McClain & Malanotte-Rizzoli, 1986; McClain *et al.*, 1986; Muller-Karger, McClain & Richardson, 1988; Muller-Karger *et al.*, 1989).

Photosynthetic pigments selectively absorb blue light and are neutral in the green. Water masses whose reflectance is determined by photosynthetic pigment absorption are called 'Case I' waters (Morel & Prieur, 1977). In 'Case II' water, suspended particulates and dissolved organic matter (DOM, yellow substance or *gelbstoff*) determine the reflectance. The water reflectance, $R(\lambda)$, is defined as the ratio of upwelling irradiance to downwelling irradiance just beneath the surface, E_u (λ, 0)/E_d (λ, 0). Because the subsurface upwelling light field is approximately Lambertian, E_u (λ, 0) $\simeq \pi^* L_u$ (λ, 0), where L_u (λ, z) is the upwelling subsurface radiance. The absorption peak for chlorophyll-a, the most important photosynthetic pigment, is 443 nm and the null point in the spectra between 520 and 550 nm is called the 'hinge point' as illustrated by stations C98, D10 and D23 in Fig. 2. Therefore, as concentration increases, the slope of the reflectance spectrum transitions from negative to positive in Case I water. In Case II water, the reflectance spectra are not as easily characterized. The bio-optical algorithm used in the global processing (Fig. 3) employs two empirical relationships, each relating the ratio of two water-leaving radiances (the upwelling radiances just above the air–water interface) to pigment concentration, L_w (443)/L_w (550) for concentration $\leq$ 1.5 mg/m^3 and L_w (520)/L_w (550) for higher concentrations (Gordon *et al.*, 1983*a*). The subsurface and water-leaving

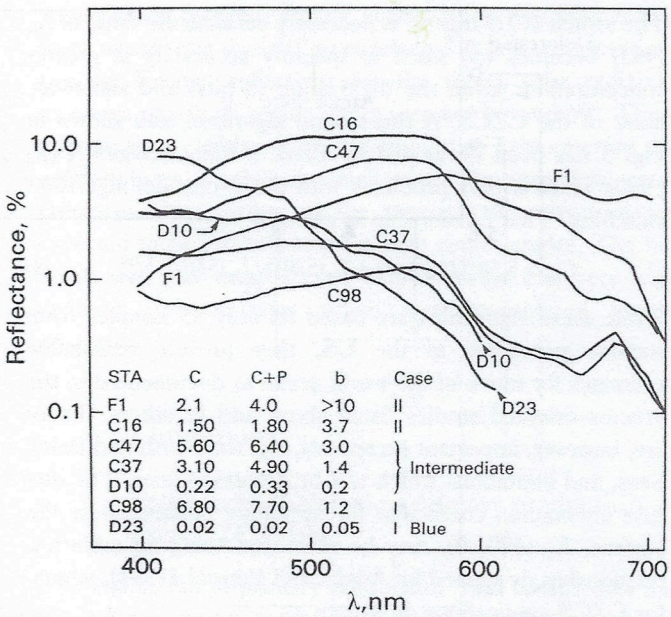

Fig. 2. Seven illustrative reflectance spectra, E_u (λ, 0) / E_d (λ, 0) (redrawn from Morel, 1980). Note that the reflectance is plotted on a logarithmic scale. C and C+P are the total water column chlorophyll-a and chlorophyll-a + phaeophytin-a concentrations, respectively. b is the average scattering coefficient at 550 nm.

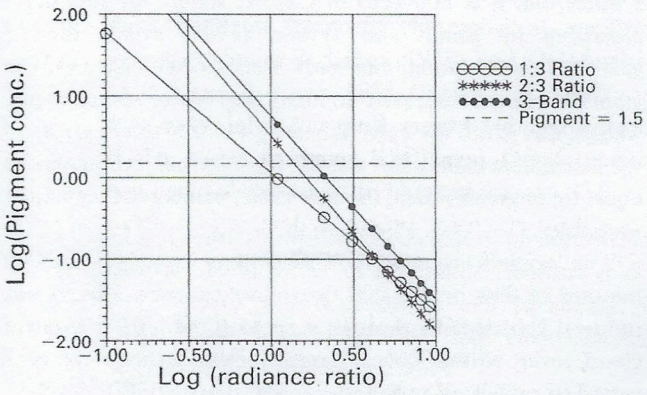

Fig. 3. Log-log plot of '2-band' and '3-band' ratio pigment algorithms. The 'Pigment = 1.5' dashed line denotes the 'switch' concentration for the 1:3 and 2:3 ratio algorithms.

radiances are proportional, and the proportionality coefficient is wavelength independent, so it cancels out in the radiance ratios. The relationships are given by

$$C_{sat} = 1.13^*[L_w(443)/L_w(550)]^{-1.71},\ 0 < C_{sat} \leq 1.5\ \text{mg/m}^3 \quad (2)$$

and

$$C_{sat} = 3.33^*[L_w(520)/L_w(550)]^{-2.44},\ 1.5\ \text{mg/m}^3 < C_{sat}. \quad (3)$$

The switch at 1.5 mg/m^3 is necessary because the value of L_w (443) becomes too small to quantify accurately at greater concentrations given the digitization (8 bits) and signal-to-noise of the CZCS. A three-band algorithm also shown in Fig. 3 has been developed by Clark (Muller-Karger *et al.*, 1990) which avoids problems with the 2-channel algorithm switching. That relationship is given by

$$C_{sat} = 5.56*[(L_w(443) + L_w(520))/L_w(550)]^{-2.252}. \quad (4)$$

While these algorithms are based on only 55 samples from stations proximate to the US, they provide reasonable estimates for much of the world ocean as documented in the process-oriented studies listed above and in others. There are, however, important exceptions, e.g. the North and Baltic Seas, and limitations which will be discussed later. The diffuse attenuation coefficient for upwelling radiance near the surface, K_u (490, 0), may be estimated using an empirical relationship developed by Austin and Petzold (1981), which, for CZCS applications, is written as

$$K_u(490,0) = 0.0883*[L_w(443)/L_w(550)]^{-1.491} + 0.022. \quad (5)$$

The final level-2 product, aerosol radiance at 670 nm, L_a (670), is obtained by assuming that L_w (670) is zero, so L_a (670) is simply the difference between the total radiance and the Rayleigh radiance. L_w (670) is approximately zero in Case I water, but it is non-zero in Case II water. An alternative algorithm by Smith and Wilson (1981) avoids the L_w (670) = 0 assumption, but only works where L_w (443) is somewhat larger than zero. In many near-shore and estuarine waters, this is not the case. When L_w (443) is small, errors in the instrument calibration and the Rayleigh correction may be equal to, or greater than, the true value, making the technique unusable.

The original volume of CZCS data (roughly 250 000 minutes of data or 125 000 two-minute scenes, Fig. 4) was reduced substantially through screening the level 0 data for cloud cover, so that only reasonably clear scenes were converted to calibrated radiance computer tapes (CRT, level 1). The screening was performed by the project scientist, Warren Hovis, shortly after the data were received. Even then, the data set filled over 30 000 1600 bpi CRTs with a final volume of approximately 700 gigabytes. The data were partitioned into scenes, usually two minutes (970 scan lines) in length. A major component of the global processing was the duplication of data from tape to write-once-read-many (WORM) optical disks which provide much greater data accessibility and media stability than magnetic tape. The processing included the creation of geophysical products in scanner coordinates (level 2) and average geophysical fields on a uniform global grid (level 3). There were three other major components to the

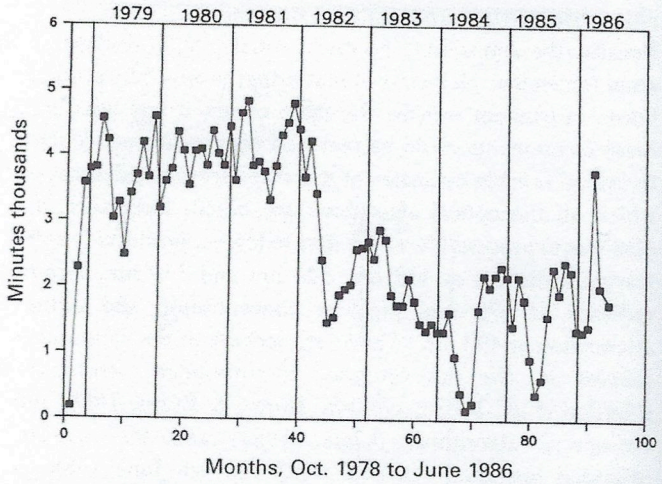

Fig. 4. Monthly total minutes of level-0 data collected by the Coastal Zone Color Scanner prior to cloud cover screening.

global processing effort: sensor calibration, quality control of the level 2 products and the archive and distribution system development. The archive is described in Feldman *et al.* (1989).

The CZCS lost sensitivity throughout the mission, but was temporally and spectrally erratic. A loss of sensitivity results in erroneously low estimates of total radiance measured by the sensor which can be compensated by adjusting the sensor calibration. There were several early attempts to quantify it (Gordon *et al.*, 1983*b*; Hovis, Knoll & Smith, 1985; Mueller, 1985; Sturm, 1986) using both direct intercomparisons with shipboard and aircraft data and indirect or 'vicarious' methods. However, as the global processing proceeded, it became clear that a more robust calibration would be required. A rigorous vicarious calibration was developed by Robert Evans at the University of Miami. The technique assumes that the normalized water-leaving radiances ($[L_w]_N(\lambda)$; Gordon & Clark, 1981) of the central gyres did not change significantly with time. By preprocessing large quantities of data and analyzing frequency distributions of the $[L_w]_N(\lambda)$s from the central gyres for each sensor gain, the drift from nominal values was quantified which provided a means for incrementally adjusting the calibration. By the end of the mission, the degradations at 443, 520, 550 and 670 nm were estimated to be $\simeq$ 40%, 20%, 15% and 10%, respectively. This approach works well for 520 and 550 nm, but is less reliable for 443 nm because of the wide range of water-leaving radiances observed in 'clear' water (Gordon & Clark, 1981).

The quality control of the level 2 products was performed at the GSFC/Laboratory for Oceans. Some scenes were automatically rejected at tape ingest for particular problems,

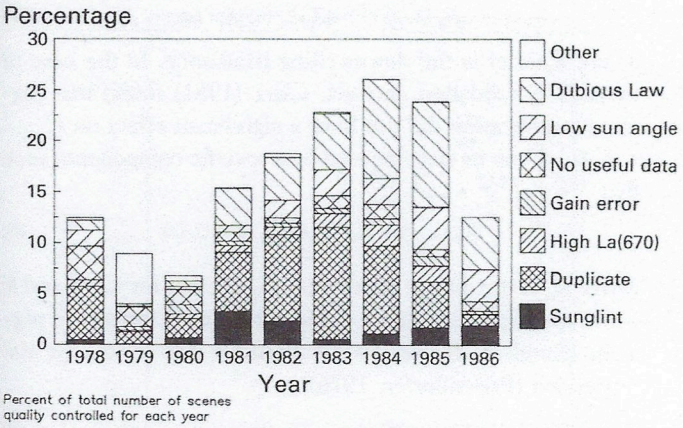

Fig. 5. Annual percentage of level-2 scenes rejected as a result of the CZCS global processing quality control effort. Rejections are quantified by rejection criteria.

e.g. missing bands. The level 2 processing also employed a land/cloud mask based on a fixed value of band 5 counts and a sensor ringing mask. Sensor ringing occurs on the downscan side of bright targets such as clouds and highly reflective land masses and results in invalid total radiances and derived products (Mueller, 1988). Special software was incorporated into the University of Miami DSP system which allowed an interactive quality control by the processing team. The procedure simultaneously displayed the daily global composites of pigment, $[L_w]_N(443)$, $[L_w]_N(550)$ and $L_a(670)$ and allowed for sequencing through each daily mosaic of scenes with the cursor. Thus, each scene was either accepted or rejected and, if rejected, one of nine rejection criteria was selected with optional comments by the investigator. The six most important categories of scene rejection, in decreasing order, were duplicate scenes, 'dubious' normalized radiances, low Sun elevation, no useful data, sunglint contamination and high L_a (670). Of nearly 62 000 scenes reviewed, over 9000 were rejected and the results are shown in Fig. 5. The duplicate scenes were due to the creation of multiple copies of the CRTs which were kept by the Nimbus Project in the tape archive. Most scenes rejected for 'dubious' normalized radiance had large areas where $[L_w]_N(550)$ was less than half the nominal value of 0.30 mW/cm^2.μm.sr that were not clearly the result of sunglint or atmospheric dust. Sunglint and dust both produce high L_a (670) values. Sunglint can be distinguished from dust because of the consistent pattern it produces in the center of equatorial scenes. A sunglint mask was applied in the level 2 processing, but the mask did not always cover the entire area of contamination because the sunglint pattern is wind speed dependent and the mask algorithm used a constant 6 m/s wind. The 'no useful data' classification was used when a scene was over land or completely cloud covered. Finally, scenes where the solar zenith angle was greater than 60° were rejected as 'low sun elevation' because Fresnel reflectivity for the direct solar radiation increases rapidly as zenith angles increase beyond 60°. Thus, at large solar zenith angles, the amount of light entering the water column is relatively small as are the upwelling water radiances. Also, errors in the atmospheric correction are expected to be greatest at these high zenith angles. The net result was that these scenes almost always had very high pigment concentrations which were considered to be erroneous.

Limitations

Estimation of biological primary productivity from CZCS data

The estimation of primary production from CZCS data has much appeal, but is not straightforward. To estimate primary production from CZCS data, the satellite pigment concentration must be related to total water column chlorophyll-a content which is, in turn, related to total water column primary production. The major limitations are due to the following.

1. The subsurface reflectance, $R(\lambda)$, in the visible spectrum results from absorption by water, photosynthetic pigments (primarily chlorophyll-a), ancillary pigments (Smith & Baker, 1978) and DOM (Bricaud, Morel & Prieur, 1981; Carder *et al.*, 1989) and scattering by water and suspended particulates (Clark, Baker & Strong, 1980) and, therefore, R is not always dominated by chlorophyll.

2. The specific absorption coefficient of phytoplankton can vary by an order of magnitude (Kishino *et al.*, 1985, 1986) and depends on cell packaging of chloroplasts, light adaptation and environmental stresses (e.g. nutrient depletion).

3. The concentration estimate derived from the CZCS, C_{sat}, is an optically weighted average over the first optical depth (Clark, 1981; Smith, 1981) of the water column and is a function of the vertical distribution of pigment concentration.

4. Subsurface maxima are common in the ocean, but are not sensed by the CZCS (Platt & Herman, 1983).

5. The relationship between chlorophyll concentration and primary production varies with species and a number of environmental and physiological condi-

tions (Smith, Eppley & Baker, 1982; Eppley *et al.*, 1985; Campbell & O'Reilly, 1988; Platt & Sathyendranath, 1988; Balch, Abbott & Eppley, 1989*a*, Balch, Eppley & Abbott, 1989*b*).

Because many substances selectively absorb light at the same wavelengths as chlorophyll, the limited number of CZCS bands does not accommodate the separation of photosynthetically active species from the others. Therefore, C_{sat} is a weighted average of all chemical species, the weight being a function of a_i, where a_i is the specific absorption coefficient. Because many of the photo-active chemical constituents are not simply dissolved, but are contained in living and nonliving particulates, a_is are often quantified in terms of bulk values with labels such as 'detritus' and 'phytoplankton', although some studies have distinguished the coefficients by phytoplankton species. In Case I water, chlorophyll and other co-varying degradation products, e.g. phaeophytin, determine the reflectance. This high correlation between chemical species allows a much higher accuracy (within ±30%; Gordon *et al.*, 1982) in pigment estimation. In Case II water, terrestrial materials, e.g. *gelbstoff* and suspended sediments, which are not necessarily correlated to chlorophyll, are important and the pigment retrievals may be grossly in error depending on the particular situation. In some coastal regions, the pigment retrievals can be quite good (Barale *et al.*, 1986; McClain *et al.*, 1988), while in others, they are poor, e.g. the Chesapeake Bay. Case II water is not necessarily synonymous with the coastal zone. For instance, coccolithopores, an open ocean phytoplankton, can have very extensive blooms which, because of their production of coccoliths (detached $CaCO_3$ platelets), produce anomalously high reflectances (Holligan *et al.*, 1983); thus, the pigment concentrations in these blooms are not quantified very well with the existing CZCS algorithms. As more data on the absorption and scattering properties are collected, better models of the water reflectance spectrum are being developed (Carder *et al.*, 1986; Gordon *et al.*, 1988; Morel, 1988).

C_{sat} is not only a composite pigment, but, being derived from the $L_w(\lambda)$s, it is also an optically weighted concentration over a portion of the upper water column from which the light is being reflected (Gordon & Clark, 1980). The depth from which 90% of the upwelling radiance originates is called the effective penetration depth, z_{90} (λ) (Gordon & McCluney, 1975). $C_{sat}(\lambda)$ is

$$C_{sat}(\lambda) = \int_0^{z_{90}(\lambda)} C(z) f(\lambda, z)\,dz \Big/ \int_0^{z_{90}(\lambda)} f(\lambda, z)\,dz \qquad (6)$$

where $f(\lambda, z) = \exp[-2K(\lambda, z)]$. Thus, $z_{90}(\lambda)$ and $C_{sat}(\lambda)$ depend on the vertical distribution of the diffuse attenuation coefficient for downwelling irradiance, $K_d(\lambda, z)$, defined as

$$K_d(\lambda, z) = -d(\ln E_d(\lambda, z))/dz \qquad (7)$$

where $E_d(\lambda, z)$ is the downwelling irradiance. In the case of the CZCS validation data set, Clark (1981) found that pigment stratification did not have a significant effect on C_{sat}.

$K_d(\lambda, z)$ can be decomposed into specific components such that

$$K_d(\lambda, z) = K_w(\lambda) + \Sigma k_i(\lambda) * C_i(z) \qquad (8)$$

where K_w is the diffuse attenuation coefficient for water and k_i is the specific attenuation coefficient for each individual pigment (Smith & Baker, 1978). k_i and a_i are related by the expression (Prisendorfer, 1976)

$$k_i = [a_i(a_i + b_i)]^{1/2} \qquad (9)$$

where b_i is the backscattering coefficient of the organism or particle. For most phytoplankton, coccolithopores being an exception, $a_i >> b_i$, so $k_i \simeq a_i$.

For vertically uniform distributions of diffuse attentuation, $z_{90}(\lambda) = 1/K_d(\lambda)$. Gordon and Morel (1983) provide relationships for $K_d(\lambda)$ as a function of pigment concentration which allow $z_{90}(\lambda)$ to be estimated. For example, in Case I water, z_{90} (443) ranges from nearly 40 meters at 0.04 mg/m^3 (the minimum concentration quantified in the global CZCS processing) to less than 1 meter at 40 mg/m^3. Because $z_{90}(\lambda)$ varies substantially with λ, the integrations implicit in the radiance ratios used in the bio-optical algorithms have different limits. However, because L_w (550) is insensitive to pigment concentration, the effect is primarily contained in the L_w (443) and L_w (520) factors.

In the open ocean, a deep chlorophyll maximum (DCM) is generally found (Cullen & Eppley, 1981; Lewis, 1987). It is not necessarily coincident to a biomass maximum or to the base of the mixed layer. Platt and Herman (1983) examined data from the Arctic, Scotian shelf and Peruvian coast and found that C_{sat} accounts for only 3–5% of the total chlorophyll in the water column. However, the percentage was fairly constant. They also found that the fraction of primary production within the effective penetration depth was even more stable at 11%. Campbell and O'Reilly (1988) analyzed the Marine Resources Monitoring, Assessment and Prediction (MARMAP) program data (over 1000 stations) from the north-east US continental shelf and slope and found the following relationship between C_{sat} and the mean concentration in the water column ($r^2 = 0.93$),

$$\langle C \rangle = 0.287 + 0.685 * C_{sat} \qquad (10)$$

Kuring *et al.* (1990) examined MARMAP and CZCS data from 1979 and compared C_{sat} with the *in situ* estimate of C_{sat} derived from ship data. They found the *in situ* values to be

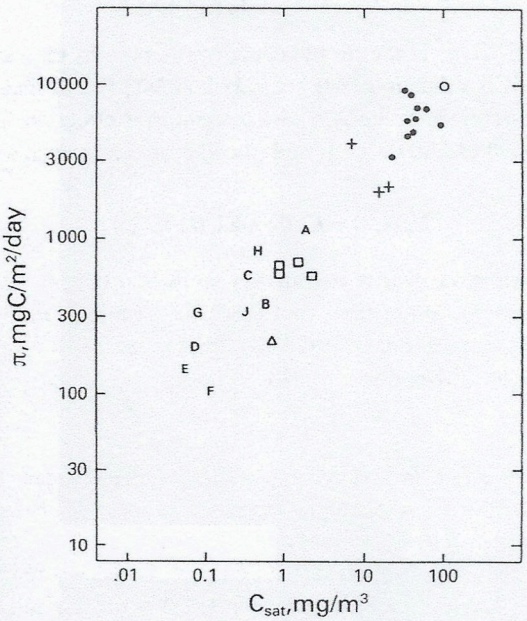

Fig. 6. Primary production, π (mgC/m²/day) data (redrawn from Eppley *et al.*, 1985). Symbols represent data from the following locations: A (Peru; June 1969), • (Peru; April 1969), + (Peru; March 1966), B (Scotia Sea), C (Panama Basin), D–G (North Pacific subtropical gyre), H (California Current), J (Lake Tahoe), Δ (Canadian Arctic, summer average), □ (Southern California bight, four seasonal averages), ○ (estimated maximum value).

roughly twice those estimated from the satellite, but could not identify a specific reason for the difference.

The correlation between C_{sat} and other mean properties of the euphotic zone provides a basis for empirical relationships between C_{sat} and total integrated primary productivity. Eppley *et al.* (1985) found that $\Pi \simeq F^{*}C_{sat}^{\frac{1}{2}}$ ($\langle F \rangle = 1000$) from data collected from a variety of oceanic regimes and seasons (Fig. 6). The Campbell and O'Reilly data set ($\langle \Pi \rangle = 914$ mg C/m²/day) is consistent with the Eppley *et al.* relationship although their values span a much smaller range of productivity and show a great deal of scatter. Eppley *et al.* examined data from the Southern California Bight and found that F has a strong seasonal dependence with maximal values in the summer and minimal values in the winter.

While empirical relationships are useful, they do not identify the underlying relationships between the physical environment and plant physiology which regulate primary production. Detailed models which explicitly incorporate parameters such as vertical biomass distribution, insolation, photoadaptation and other quantities are called photosynthesis–light (P–L) models. These models are somewhat different from biomass models which estimate the balance between phytoplankton, zooplankton and nutrient concentrations (P–Z–N models). Satellite pigment fields have been used to qualitatively validate P–Z–N models (Wroblewski, Sarmiento & Flierl, 1988), but these models will not be discussed here. A detailed examination of several empirical and semi-analytical Π algorithms is provided in Balch *et al.* (1989*a*, *b*). One P–L model oriented towards satellite applications is described in Platt *et al.* (1988) and Platt and Sathyendranath (1988). Their approach requires certain information on the vertical distribution of biological quantities and physiological rate parameters as a function of season and location. Once oceanic regions are classified and assigned parameter values based on *in situ* observations, the modelled production can be calculated. Their initial results for five sites in the north and east Atlantic show excellent correlation to observed values over the entire range of their observation data set (0 to 2500 mg C/m²/day). However, Balch *et al.* (1989*b*) argue that the variability of the photosynthesis–light relationship is much greater than Platt *et al.* (1988) concluded.

Analysis and results

Abbott and Chelton (1990) provide a comprehensive review of the literature dealing with applications of CZCS data. Nearly all of the current literature is related to either algorithm or regional process studies. However, the CZCS data set has provided the first truly comprehensive view of the global ocean's pigment and radiance fields. Fig. 7(*a*) is the average pigment field derived from the entire 7.7-year data set. A comparison with the *in situ* composites of productivity (Berger, 1989) indicate an amazingly close correspondence in patterns. It must be noted that the sampling was extremely inhomogeneous in time and space as illustrated in Figs. 4 and 7(*b*), respectively. Fig. 7(*b*) is a map of the total number of samples used to compute the mean values in Fig. 7(*a*). These numbers are not the total number of samples actually collected by the satellite, but are the number of samples remaining after the initial cloud screening, subsampling for global processing and quality control. Sampling was highly localized because of the Nimbus experiment team's sampling priorities and solar elevation and cloud cover conditions. Other factors that limited the amount of data collected were ground station availability, tape recorder capacity, satellite power limitations and, in the latter phase of the mission, difficulties in getting the instrument to switch on. The highest value in Fig. 7(*b*) is roughly 16 000, but most values are less than 400. The greatest numbers of valid pixels were from the east (Florida to Maine) and west (Baja to Washington state) coasts of North America, the western Mediterranean Sea and the Arabian Sea. It must be mentioned that as a proof-of-concept mission,

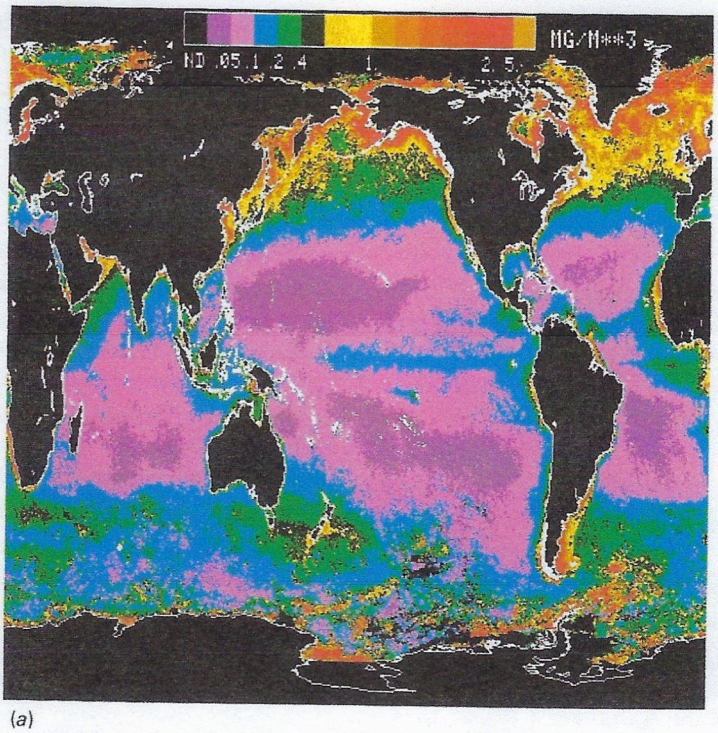

(*a*)

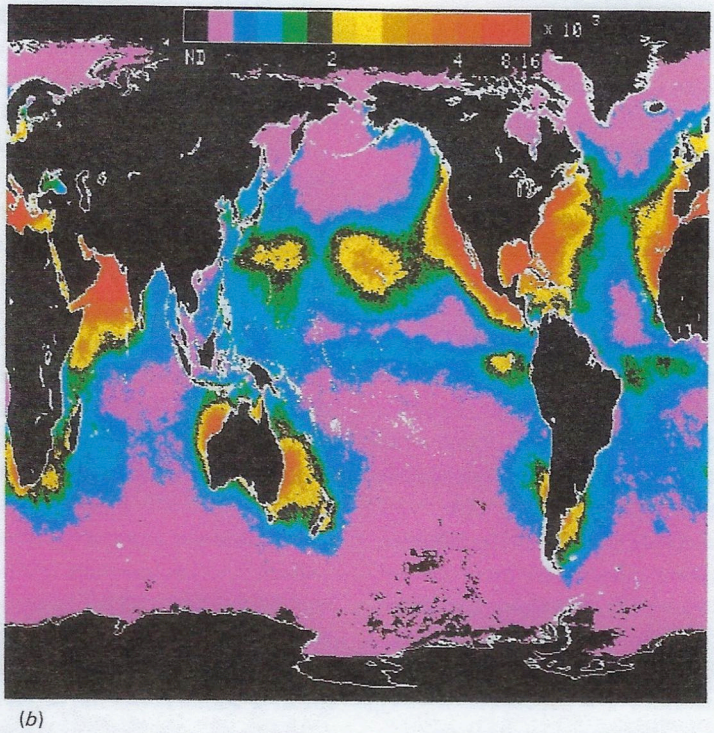

(*b*)

Fig. 7. (*a*) Overall mean CZCS pigment field for entire data set (November 1978 through June 1986) and (*b*) total number of valid samples processed.

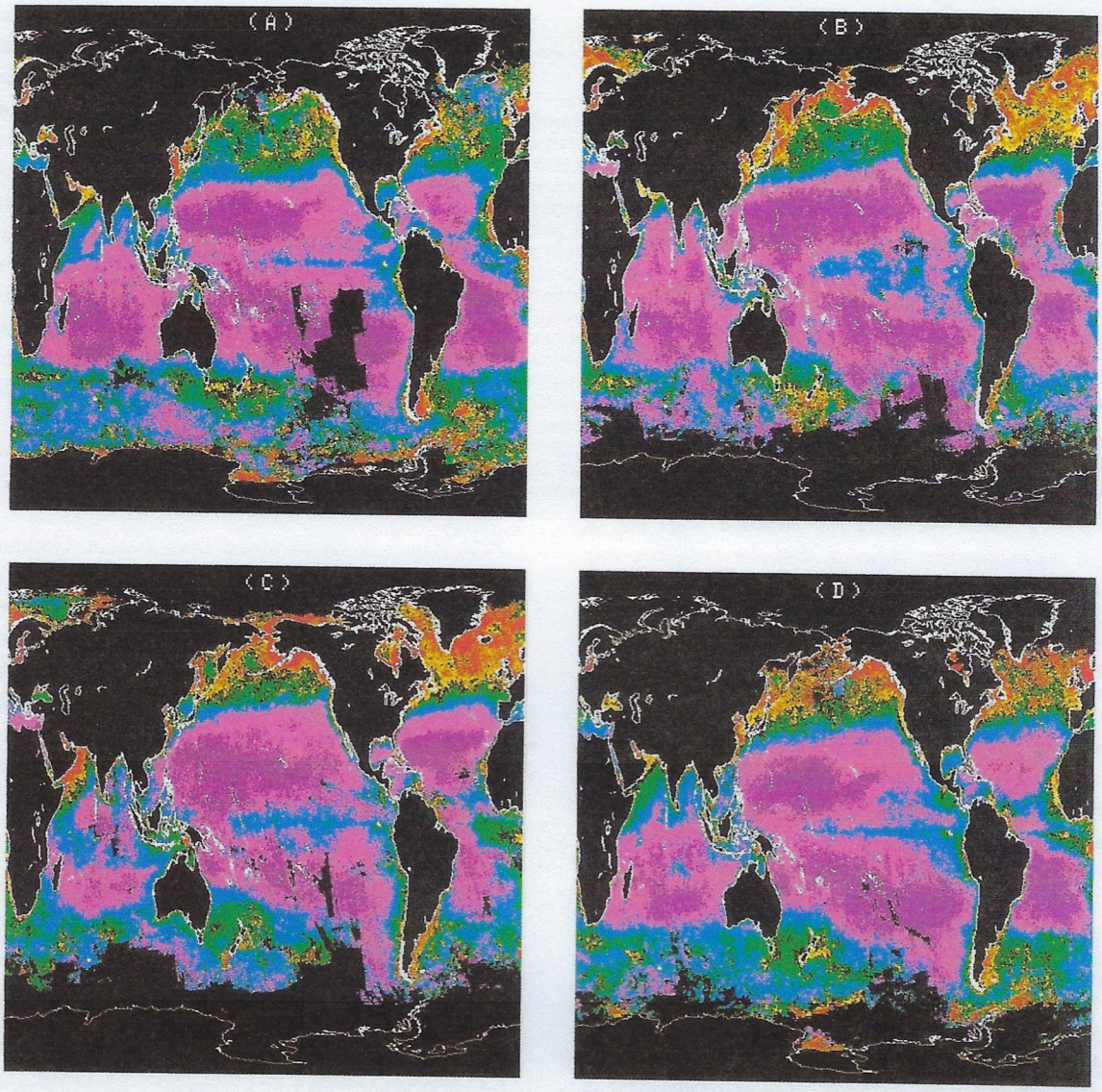

Fig. 8. Seasonal mean CZCS pigment fields (A) Winter: January through March, (B) Spring: April through June, (C) Summer: July through September, (D) Fall: October through December.

global coverage was never envisioned as a goal of the CZCS project.

The data set does provide synoptic-scale time series of surface pigment concentrations for at least those regions mentioned above. In certain instances, significant inter-annual variability (Feldman, 1986; Banse & McClain, 1986; Barale *et al.*, 1986; Brock & McClain, 1992) has been observed. For regions and periods when coverage was less dense, averaging the data into seasonal climatologies can provide a clearer picture of the seasonal cycle as in Fig. 8. Due to the uneven temporal and spatial sampling (Figs. 4 and 7(*b*)), some features in the seasonal composites are artefacts of temporally inhomogeneous sampling coupled with inter-annual variability. None the less, the seasonal cycle is clearly demonstrated in regions like the North Atlantic Ocean (McClain *et al.*, 1990). Several interesting phenomena are depicted in Fig. 8 including 1) the relative constancy of the Southern Hemisphere compared to the Northern Hemisphere, 2) the higher concentrations in the north and tropical Atlantic versus the corresponding areas of the Pacific and 3) the high productivity of the Arabian Sea during the summer monsoon (Brock *et al.*, 1991).

Some very important regions, e.g. equatorial Pacific and Atlantic Oceans, had little or no data for some important

periods. For instance, almost no data were collected in the equatorial Pacific during the 1982–1983 El Niño or the 1983–1984 period of pronounced inter-annual variability in the equatorial Atlantic (see *Nature*, 322, 17 July, 1986), yet these regions are vital to our understanding of the ocean's role in the Earth's carbon budget. The lack of periodic global coverage and questions regarding the calibration, have limited what can be inferred about long-term trends in global productivity and no analyses of the CZCS data have been published thus far that attempt to do so. An analysis of this kind is complicated by the highly non-linear relationship between C_{sat} and Π. A direct computation of Π from an image of average concentration using a relationship such as that of Eppley *et al.* (1985) would not yield satisfactory results in regions where C_{sat} has significant variability. In those situations, the transformation would need to be executed on individual scenes before averaging is performed. Also, use of an image of mean pigment assumes that the sampling was adequate to estimate the true average.

Conclusions

The global processing and archival of the CZCS data has only recently made that data set generally available to the oceanographic community and extensive analyses of the data set for the estimation of primary productivity are being pursued by a number of investigators. The CZCS data has revealed a great deal about the global ocean and clearly demonstrated the feasibility of monitoring oceanic biological processes on a global scale. Also, the experience gained from the CZCS data processing has helped clarify what refinements in sensor design are needed in the next generation of instruments. Clearly, more wavelengths are needed in order to distinquish viable chlorophyll from degradation products, to improve the aerosol correction and to accommodate a more robust suite of pigment algorithms for Case II waters. Higher signal-to-noise ratios and data quantification will allow more accurate atmospheric corrections. Also, to do global science, the coverage shown in Figs. 7 and 8 is needed on a weekly basis and process-oriented studies require daily data from experiment sites. Finally, the instrument performance must be monitored in near realtime. The only mechanism for obtaining an adequate data set to address issues of global biogeochemical cycles and global change is an *operational* ocean color satellite sensor such as SeaWiFS (Yoder *et al.*, 1988) coupled with a comprehensive calibration, validation and bio-optical algorithm development program. With large international *in situ* programs like JGOFS (joint global ocean flux study), IGBP (international geosphere–biosphere program) and WOCE (world ocean circulation experiment) already under way, the opportunity for a significant synergism between field and satellite data sets is possible for the first time. Indeed, programs like JGOFS are seriously hampered by the lack of simultaneous satellite coverage.

Availability of data

CZCS data can be obtained from NASA Goddard Space Flight Center and a number of regional archives (Feldman *et al.*, 1989). A browse capability has been developed which includes 1) software that allows the user to query a database using a number of parameters including latitude and longitude ranges and time interval to determine the scenes available which satisfy the query criteria and 2) a set of three Panasonic video disks which contain all the CZCS pigment images. The browse software can be used with or without the Panasonic player and versions are available for a variety of computers. Using the Panasonic video player allows each image that satisfies the query to be displayed and the user has the option of ordering the displayed scene before progressing to the next scene. Orders to the archive can be initiated from within the browse session provided the system is a SPAN node. Data requests may also be filed through OMNET. For information about the CZCS archive, contact DAAC User Support Office, Code 902.2, NASA/GSFC, Greenbelt, MD 20 771. Tel: (301) 286-3209. Omnet: DAAC. GSFC: SPAN, NCS; DAAC USO internet: DAAC USO QUSSD-CA.GSFC.NASA.GOV. The browse software is available at no charge.

Table 1. *Notation*

Symbol	*Units*	*Definition*
a_i	m^2/mg	Specific absorption coefficient for i_{th} optical species
b_i	m_2/mg	Specific scattering coefficient for i_{th} optical species
c_i	m^2/mg	a_i+b_i, specific attenuation coefficient
C	mg/m^3	Pigment concentration
C_{sat}	mg/m^3	Satellite-derived pigment concentration
$E_d(\lambda, z)$	$mW/cm^2 \cdot \mu m$	Downwelling irradiance
$E_u(\lambda, z)$	$mW/cm^2 \cdot \mu m$	Upwelling irradiance
f	dimensionless	*f*-ratio, ratio of new production to primary production
F	$(mg/m)^{1/2}/day$	Proportionality constant in Eppley satellite productivity relationship
k_i	m^2/mg	Specific diffuse attenuation coefficient for the i_{th} optical species
$K_d(\lambda, z)$	m^{-1}	Diffuse attenuation coefficient for downwelling irradiance
$K_u(\lambda, z)$	m^{-1}	Diffuse attenuation coefficient for upwelling radiance
$K_w(\lambda)$	m^{-1}	Diffuse attenuation coefficient for water
$L_a(\lambda)$	$mW/cm^2 \cdot \mu m \cdot sr$	Aerosol radiance
$L_u(\lambda, z)$	$mW/cm^2 \cdot \mu m \cdot sr$	Upwelling water radiance
$L_w(\lambda)$	$mW/cm^2 \cdot \mu m \cdot sr$	Water-leaving radiance above the air–sea interface
$[L_w]_N(\lambda)$	$mW/cm^2 \cdot \mu m \cdot sr$	Normalized water-leaving radiance
Π	$mg\ C/m^2/day$	Primary productivity
$R(\lambda)$	dimensionless	Reflectance
$z_{90}(\lambda)$	m	Effective penetration depth

References

Abbott, M. R. & Chelton, D. B. (1991). Advances in passive remote sensing of the ocean, U. S. National Report to International Union of Geodesy and Geophysics 1987–1990. *Contributions in Oceanography*, Am. Geophys. Union, 571–589.

Abbott, M. R. & Zion, P. M. (1985). Satellite observations of phytoplankton variability during an upwelling event, *Cont. Shelf Res.*, **4**, 661–80.

Anderson, N. R. & Malahoff, A. M. (eds.) (1977). *The Fate of Fossil Fuel CO_2 in the Oceans*, Plenum Press, New York, 749pp.

Austin, R. W. & Petzold, T. J. (1981). The determination of diffuse attenuation coefficient of sea water using the Coastal Zone Color Scanner, *Oceanography from Space*, J. F. R. Gower (ed.), Plenum Press, New York, 239–56.

Balch, W. M., Abbott, M. R. & Eppley, R. W. (1989*a*). Remote sensing of primary production – I. A comparison of empirical and semi-empirical algorithms. *Deep-Sea Res.*, **36**(2), 281–95.

Balch, W. M., Eppley, R. W. & Abbott, M. R. (1989*b*). Remote sensing of primary production – II. A semi-analytical algorithm based on pigments, temperature and light. *Deep-Sea Res.*, **36**(8), 1201–17.

Banse, K. & McClain, C. R. (1986). Satellite-observed winter blooms of phytoplankton in the Arabian Sea. *Mar. Ecol. Prog. Ser.*, **34**(3), 201–11.

Barale, V., McClain, C. R. & Malanotte-Rizzoli, P. (1986). Space and time variability of the surface color field in the northern Adriatic Sea, *J. Geophys. Res.*, **91**, 12, 957–74.

Berger, W. H. (1989). Global maps of ocean productivity, *Productivity of the Ocean: Present and Past.* (W. H. Berger, V. S. Smetacek and G. Wefer, eds.), John Wiley & Sons, New York, pp. 429–55.

Berger, W. H., Smetacek, V. S. & Wefer, G. (1989). Ocean productivity and paleoproductivity – an overview, *Productivity of the Ocean: Present and Past.* (W. H. Berger, V. S. Smetacek and G. Wefer, eds.), John Wiley & Sons, New York, pp. 1–34.

Bricaud, A., Morel, A. & Prieur, L. (1981). Absorption of dissolved organic matter of the sea (yellow substance) in the UV and visible domains. *Limnol. Oceanogr.*, **26**, 43–53.

Brock, J. C. & McClain, C. R. (1992). Inter-annual variability in phytoplankton blooms observed in the northwestern Arabian Sea during the southwest monsoon. *J. Geophys. Res.*, **97**(C1), 733–50.

Brock, J. C., McClain, C. R., Luther, M. E. & Hay, W. W. (1991). The phytoplankton bloom in the northwest Arabian Sea during the southwest monsoon of 1979. *J. Geophys. Res.*, **96**(C11), 20, 623–42.

Campbell, J. W. & O'Reilly, J. E. (1988). Role of satellites in estimating primary productivity on the northwest Atlantic continental shelf. *Cont. Shelf Res.*, 8(2), 179–204.

Carder, K. L., Steward, R. G., Paul, J. H. & Vargo, G. A. (1986). Relationships between chlorophyll and ocean color constituents as they affect remote-sensing reflectance models. *Limnol. Oceanogr.*, **31**, 403–13.

Carder, K. L., Steward, R. G., Harvey, G. R. & Ortner, P. B. (1989). Marine humic and fulvic acids: Their effects on remote sensing of ocean chlorophyll. *Limnol. Oceanogr.*, **34**(1), 68–81.

Clark, D. K. (1981). Phytoplankton pigment algorithms for the Nimbus-7 CZCS. In *Oceanography from Space*. (J. R. F. Gower, ed.,) Plenum Press, New York, pp. 227–37.

Clark, D. K., Baker, E. T. & Strong, A. E. (1980). Upwelled spectral radiance distributions in relation to particulate matter in sea water. *Boundary-Layer Meteor.*, **18**(3), 287–98.

Cullen, J. J. & Eppley, R. W. (1981). Chlorophyll maximum layers of the Southern California Bight and possible mechanisms of their formation maintenance. *Oceanol. Acta*, **4**(1), 23–32.

Deuser, W. G., Muller-Karger, F. E. & Hemleben, C. (1988). Temporal variations of particle fluxes in the deep subtropical and tropical North Atlantic: Eulerian versus Lagrangian effects. *J. Geophys. Res.*, **93**(C6), 6857–62.

Eppley, R. W. (1989). New production: history, methods, problems. In *Productivity of the Ocean: Present and Past* (W. H. Berger, V. S. Smetacek and G. Wefer, eds.), John Wiley & Sons, New York, pp. 85–97.

Eppley, R. W., Stewart, E., Abbott, M. R. & Heyman, U. (1985). Estimating ocean primary production from satellite chlorophyll: introduction to regional differences and statistics for the Southern California Bight. *J. Plankton Res.*, **7**(1), 57–70.

Esaias, W., Feldman, G., McClain, C. R. & Elrod, J. (1986). Satellite observations of oceanic primary productivity. *Eos* **67**(44), 835–7.

Falkowski, P. G. (ed.). (1980). *Primary Productivity in the Sea.* Plenum Press, New York, 531pp.

Feldman, G. (1986). Variability of the productive habitat in the eastern equatorial Pacific, *Eos*, **67**, 106–8.

Feldman, G., Clark, D. & Halpern, D. (1984). Satellite color observations of the phytoplankton distribution in the eastern equatorial Pacific during the 1982–1983 El Niño. *Science*, **226**(4678), 1069–71.

Feldman, G. *et al.* (1989). Ocean color: availability of the global data set, *Eos*, **70**(23), 634.

Global Ocean Flux Committee (1984). *Global Ocean Flux Study: Proceedings of a Workshop*, National Academy Press, Washington, DC, 360pp.

Gordon, H. R. & Clark, D. K. (1980). Remote sensing optical properties of a stratified ocean: an improved interpretation. *Appl. Opt.*, **18**, 3428–30.

Gordon, H. R. & Clark, D. K. (1981). Clear water radiances for atmospheric correction of Coastal Zone Color Scanner imagery. *Appl. Opt.*, **20**, 4175–80.

Gordon, H. R. & McCluney, W. R. (1975). Estimation of the depth of sunlight penetration in the sea for remote sensing. *Appl. Opt.*, **14**(2), 413–16.

Gordon, H. R. & Morel, A. Y. (1983). *Remote Assessment of Ocean Color for Interpretation of Satellite Visible Imagery, A Review.* Springer-Verlag, New York, 114 pp.

Gordon, H. R., Clark, D. K., Brown, J. W., Brown, O. B. & Evans, R. H. (1982). Satellite measurements of phytoplankton pigment concentration in the surface waters of a warm core Gulf Stream ring. *J. Mar. Res.*, **40**(2), 491–502.

Gordon, H. R., Clark, D. K., Brown, J. W., Brown, O. B., Evans, R. H. & Broenkow, W. W. (1983*a*). Phytoplankton pigment concentrations in the Middle Atlantic Bight: comparison of ship determinations and CZCS estimates, *Appl. Opt.*, **22**(1), 20–36.

Gordon, H. R., Brown, J. W., Brown, O. B., Evans, R. H. & Clark, D. K. (1983*b*). Nimbus-7 CZCS: reduction of its radiometric sensitivity with time, *Appl. Opt.*, **22**(24), 3929–31.

Gordon, H. R., Brown, J. W. & Evans, R. H. (1988). Exact Rayleigh scattering calculations for use with the Nimbus-7 Coastal Zone Color Scanner, *Appl. Opt.*, **27**(5), 862–71.

Holligan, P. M., Viollier, M., Harbour, D. S., Camus, P. & Champagne-Phillippe, M. (1983). Satellite and ship studies of coccolithopore production along a continental shelf edge. *Nature*, **304**, 339–42.

Hovis, W. A. (1981). The Nimbus-7 Coastal Zone Color Scanner (CZCS) program, *Oceanography from Space.* (J. R. F. Gower, ed.), Plenum Press, New York, pp. 213–25, 1981.

Hovis, W. A., Knoll, J. S. & Smith, G. R. (1985). Aircraft measurements for calibration of an orbiting spacecraft sensor. *Appl. Opt.*, **24**(3), 407–10.

Kishino, M., Okami, N., Takahashi, M. & Ichimura, S. (1986). Light utilization efficiency and quantum yield of phytoplankton in a thermally stratified sea. *Limnol. Oceanogr.*, **31**(3), 557–66.

Kishino, M., Takahashi, M., Okami, N. & Ichimura, S. (1985). Estimation of the spectral absorption coefficients of phytoplankton in the sea. *Bull. Mar. Sci.*, **37**, 634–42.

Kuring, N., Lewis, M. R., Platt, T. & O'Reilly, J. E. (1990). Satellite-derived estimates of primary production on the northwest Atlantic continental shelf. *Cont. Shelf Res.*, **10**(5), 461–84.

Lewis, M. R. (1987). Phytoplankton and thermal structure in the tropical ocean, *Oceanol. Acta*, **SP**, 91–5.

McClain, C. R., Pietrafesa, L. J. & Yoder, J. A. (1984). Observations of Gulf Stream-induced and wind-driven upwelling in the Georgia Bight using ocean color and infra-red imagery, *J. Geophys. Res.*, **89**, 3705–23.

McClain, C., Chao, S.-Y., Atkinson, L., Blanton, J. & de Castillejo, F. (1986). Wind-driven upwelling in the vicinity of Cape Finisterre, Spain. *J. Geophys. Res.*, **91**(C7), 8470–86.

McClain, C. R., Yoder, J. A., Atkinson, L. P., Blanton, J. O., Lee, T. N., Singer, J. J. & Muller-Karger, F. (1988). Variability of Surface Pigment Concentrations in the South Atlantic Bight, *J. Geophys. Res.*, **93**(C9), 10, 675–97.

McClain, C. R., Esaias, W. E., Feldman, G. C., Elrod, J., Endres, D., Firestone, J., Darzi, M., Evans, R. & Brown, J. (1990). Physical and biological processes in the North Atlantic during the First Global GARP Experiment. *J. Geophys. Res.*, **95**(C10), 18,027–48.

Moore, B., III & Bolin, B. (1986). The oceans, carbon dioxide, and global climate change. *Oceanus*, **29**(4), 9–15.

Morel, A. (1980). In-water and remote measurements of ocean color, *Bound.-layer Meteorol.*, **18**(2), 178–201.

Morel, A. (1988). Optical modeling of the upper ocean in relation to its biogenous matter content (Case I waters). *J. Geophys. Res.*, **93**(C9), 10,749–68.

Morel, A. & Prieur, L. (1977). Analysis of variations in ocean color, *Limnol. Oceanogr.*, **22**, 709–22.

Mueller, J. L. (1985). Nimbus-7 CZCS: confirmation of its radiometric sensitivity decay rate through 1982. *Appl. Opt.*, **24**(7), 1043–7.

Mueller, J. L. (1988). Nimbus-7 CZCS: electronic overshoot due to cloud reflectance. *Appl. Opt.*, **27**(3), 438–40.

Mueller-Karger, F., McClain, C. R. & Richardson, P. (1988). The dispersal of the Amazon water. *Nature*, **333**, 56–9.

Muller-Karger, F. E., McClain, C. R., Fisher, T. R., Esaias, W. E.

& Varela, R. (1989). Pigment distribution in the Caribbean Sea: observations from space. *Prog. Oceanog.*, **23**, 23–64.

Muller-Karger, F. E., McClain, C. R., Sambrotto, R. N. & Ray, G. C. (1990). A comparison of ship and CZCS-mapped distributions of phytoplankton in the Southeastern Bering Sea, *J. Geophys. Res.*, **95**(C7), 11,483–99.

Platt, T. & Herman, A. W. (1983). Remote sensing of phytoplankton in the sea: surface-layer chlorophyll as an estimate of water-column chlorophyll and primary production. *Int. J. Remote Sensing*, **4**(2), 343–51.

Platt, T. & Sathyendranath, S. (1988). Oceanic primary production: estimation by remote sensing at local and regional scales. *Science*, **241**, 1613–20.

Platt, T., Sathyendranath, S., Caverhill, C. M. & Lewis, M. R. (1988). Ocean primary production and available light: further algorithms for remote sensing. *Deep-Sea Res.*, **35**(6), 855–79.

Prisendorfer, R. W. (1976). *Hydrologic Optics, Volume V. Properties.* US Dept. of Commerce, 296pp.

Smith, R. C. (1981). Remote sensing and depth distribution of ocean chlorophyll. *Mar. Ecol. Prog. Ser.*, **5**, 359–61.

Smith, R. C. & Baker, K. S. (1987*b*). Optical classification of natural waters. *Limnol. Oceanogr.*, **23**(2), 260–7.

Smith, R. C. & Wilson, W. H. (1981). Ship and satellite bio-optical research in the California Bight, *Oceanography from Space.* (J. F. R. Gower, ed.), Plenum Press, New York, pp. 281–294.

Smith, R. C., Eppley, R. W. & Baker, K. S. (1982). Correlation of primary productivity as measured aboard ship in southern California coastal waters and as estimated from satellite chlorophyll images, *Mar. Biol.*, **66**, 281–8.

Strum, B. (1986). Correction of the sensor degradation of the Coastal Zone Color Scanner on Nimbus-7. *ESA SP-258*, 263–7.

Sundquist, E. T. & Broecker, W. S. (eds.) (1985). *The Carbon Cycle and Atmospheric CO_2 Natural Variations Archean to Present*, American Geophysical Union, Washington, DC, 627pp.

Tans, P. P., Fung, I. Y. & Takahashi, T. (1990). Observational constraints on the global atmospheric CO_2 budget, *Science*, **247**, 1431–8.

Wroblewski, J. S., Sarmiento, J. L. & Flierl, G. R. (1988). An ocean basin scale model of plankton dynamics in the North Atlantic 1. solutions for the climatological oceanographic conditions in May, *Global Biogeochem. Cycles*, **2**(3), 199–218.

Yoder, J. A., Esaias, W. E., Feldman, G. C. & McClain, C. R. (1988). Satellite ocean color – status report. *Oceanography Magazine*, **1**(1), 18–20.